

Catalysis

Tuning the Synthetic Parameters to Obtain Smart C-N Co-Doped Titania Photocatalysts for NO_x AbatementA. Olivo,^[a] M. Signoreto,^[a] E. Ghedini,^{*[a]} F. Pinna,^[a] D. Marchese,^[a] Prof. M. Signoreto,^[a] G. Cruciani,^[b] and M. Manzoli^[c]

Global society is constantly seeking for sustainable and effective processes to fight environmental pollution. The abatement of NO_x, a class of hazardous contaminants, can be performed by means of photocatalytic oxidation using titania-based photocatalysts. Non-metal doping is highly desirable for an efficient exploitation of solar light. The co-presence of nitrogen and carbon represents an appealing possibility though their introduction generally requires post-synthesis treatments.

Otherwise, in this work carbon and nitrogen have been introduced in titania photocatalysts simultaneously by a one-pot synthetic approach using a natural and sustainable source of dopants, namely chitosan. Several synthetic parameters have been changed in order to evaluate their effect on the physicochemical properties of the final materials and to establish structure-activity relationship as for the photocatalytic performances in NO_x oxidation under visible light irradiation.

Introduction

Driven by intergovernmental concern about NO_x noxious effects on mankind and environment, the scientific community is continuously searching for new technologies that are able to provide better air quality and, at the same time, to keep the pace with the increasing strictness of international regulations. Alongside selective catalytic reduction (SCR) and photocatalytic reduction (PCR), photocatalytic oxidation (PCO) is recognized as one of the most promising processes to abate NO_x emissions.^[1,2] The preferred photocatalyst for NO_x abatement is titania, due to its large availability, low cost and wide applicability in many fields, especially in paintings and green building industry.^[3-5] Unfortunately, the main titania drawback is its relatively large band gap (3.2 eV in anatase phase, corresponding to about 25770 cm⁻¹),^[6] which does not allow an efficient exploitation of solar light, a natural and renewable source of energy. Actually, UV light is only ca. 5 % of total solar radiation.^[7] To increase visible light response, several approaches have been pursued aimed at red-shifting the titania absorption. Among possible methods, the introduction of a sensitizer (usually an organic dye) on the photocatalytic surface has been reported.^[8-10] Another possibility to improve photoactivity under visible light

is to promote titania with non-metal dopants, such as nitrogen,^[11,12] carbon,^[13] sulphur,^[14] fluorine^[15] and iodine.^[16] TiO_{2-x}N_x was synthesized firstly by Asahi and co-workers in 2001 and opened the field to the so-called *visible light active photocatalysts*.^[17] The same researchers also reported that nitrogen, in order to be an effective dopant, has to substitute oxygen in the titania lattice.^[18] A substitutional doping introduces localized N 2p orbitals slightly above the semiconductor valence band. Afterwards, Di Valentin et al. found that also interstitial nitrogen, due to its π*N-O orbitals, is able to red-shift the titania light absorption capability.^[19] The nature of nitrogen in the final N-doped photocatalysts is strictly dependent on the synthetic approach.^[20] Another effective dopant for titania is carbon.^[21-23] This element can be introduced on titania photocatalysts in different ways, such as flame pyrolysis,^[24] chemical vapour deposition,^[25] and the use of organic compounds (e.g. exane^[26]). Recently, attention has been shifted on more sustainable carbon sources, like glucose.^[27] Depending on its source, carbon can be displayed either as a substitutional anion or as an interstitial cation.^[28,29] In the former case, Ti-C bond is observed, while in the latter one C-O (carbonate) bond is more likely.^[30,31] Nonetheless, Kirsh et al reported that carbon efficiency is not due to a modification of titania lattice, but carbon species, differently from nitrogen, act as sensitizers, injecting electrons from the dopant to the conduction band of titania.^[32] In order to increase the doping effectiveness, co-doping has been intensively investigated due to its greater effectiveness compared to single doped catalysts. Chen et al. supposed a synergy between the dopants that provides a beneficial effect on visible light photoactivity.^[33] Though acting in different ways, both carbon and nitrogen enhance the formation of electron-hole excited pairs under visible light irradiation. Several methods have been pursued to synthesise C-N co-doped titania photocatalysts. Generally, carbon and nitrogen are introduced on titania in post-synthesis treatments.^[34-37] Recently, we reported synthetic procedures in which

[a] A. Olivo, M. Signoreto, Dr. E. Ghedini, Prof. F. Pinna, D. Marchese, P. M. Signoreto
Dept. of Molecular Sciences and Nanosystems
Ca' Foscari University Venice and Consortium INSTM, RU of Venice
Via Torino 155, 30172 Venezia, Italy
E-mail: gelena@unive.it

[b] Prof. G. Cruciani
Dept. of Physics and Earth Sciences
University of Ferrara
Via G. Saragat 1, I-44122 Ferrara, Italy

[c] Dr. M. Manzoli
Dept. of Drug Science and Technology & NIS Interdepartmental Centre
University of Turin
Via P. Giuria 7, 10125 Turin, Italy

only one of the dopants is introduced during the catalyst preparation, whereas the other is introduced afterwards.^[38] In very few works it is reported a one-pot synthesis that allows to synthesise the photocatalytic system and to introduce carbon and nitrogen simultaneously.^[39] The preferred carbon and nitrogen sources are alkyl ammonium compounds, such as tetrabutylammonium hydroxide.^[37] In this study, a more sustainable synthesis that employs a natural compound, such as chitosan, is proposed. This natural polyglucosamine, deriving from chitin deacetylation, has been chosen for its large availability, sustainability, low cost and the co-presence of carbon and nitrogen.^[40] Therefore, the goal of the present study is to synthesise an efficient C and N co-doped titania photocatalysts using chitosan as source of dopants. This innovative approach to dope simultaneously titania with C and N by using a natural source, at the best of our knowledge, has never been tried for photocatalytic applications and it could be a viable option for photocatalytic NO_x removal under visible light. The sol-gel process has been chosen for these purposes and several synthetic parameters have been studied in order to obtain the best C-N co-doped titania photocatalyst for NO_x oxidation.

Results and Discussion

Chitosan-free photocatalyst

The structural and morphological properties of the chitosan-free sample (T sample) and its photocatalytic activity have been investigated before considering the chitosan effect on the photocatalytic system. Titania crystalline phase is a crucial parameter for photocatalytic activity and anatase phase is highly desirable.^[41] The phase transition from amorphous titania to anatase crystal phase usually occurs between 300 °C and 400 °C.^[42] Therefore, the calcination should be performed at 350 °C to ensure the occurrence of the transition to anatase phase. In order to assess the effectiveness of the calcination treatment and to gain some preliminary information about the features of the synthesized sample (such as crystal structure and surface properties, in particular about C species), X-ray diffraction, TG-DTA and TPO analyses were resorted on.

The T sample calcined at 350 °C is exclusively made up by the anatase tetragonal phase as shown in the XRD pattern reported in Figure 1, where all the detected peaks correspond to this crystalline phase, in accordance with JCPDS card no. 00-002-0387. Anatase phase is the most suitable for photocatalytic purposes and the T sample calcined at 350 °C has been further tested in NO oxidation under visible light. Such sample showed a 32 % NO conversion. The KRONOS 7000 reference material, that has been designed to be extremely active under visible light, is approximately three times more active (90 % NO conversion). This big difference in photoactivity cannot be understood only in terms of nature of the crystalline phase, since both titania photocatalysts display the anatase crystalline structure. This means that, even if the crystal phase is a crucial requirement for obtaining efficient photocatalysts, it is not sufficient to justify the observed discrepancy in the photocatalytic behaviour and that other factors play a role in

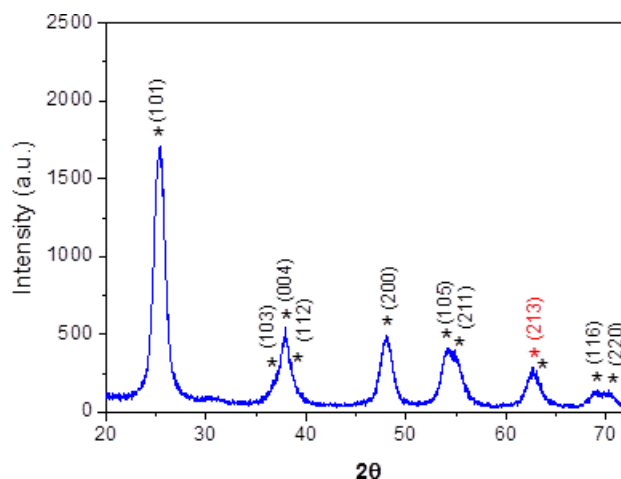


Figure 1. XRD pattern of T sample calcined at 350 °C.

determining the photoactivity. According to the patent,^[43] the increase in the activity displayed by the commercial photocatalyst is due to the presence of residual carbon from either succinic acid or pentaerythritol used as C sources. In order to understand the reasons of the poor photoactivity of the T sample with respect to that displayed by KRONOS 7000, TG-

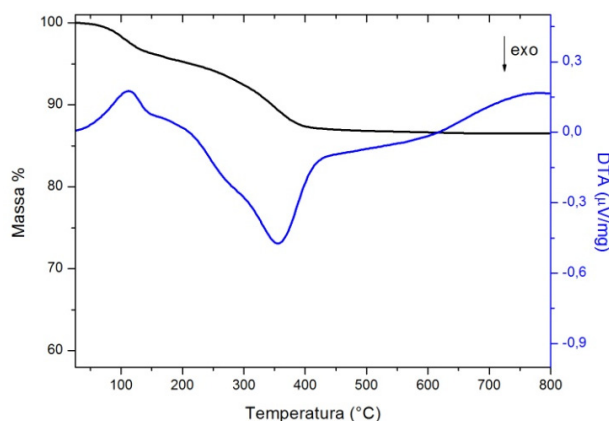


Figure 2. TG/DTA analysis for the as prepared T sample before calcination.

DTA and TPO analyses have been resorted on. Figure 2 shows the TG and DTA profiles of the as prepared T sample.

The weight loss takes place in two stages: the first one starts at 60 °C, ends at 150 °C (with a weight loss of ~10 %) and it is assigned to the endothermic loss of water. The second exothermic stage ranges between 150 and 400 °C and involves a gradual weight loss, due to the evolution of organic species derived from the synthetic procedure (such as titanium(IV) tetrabutoxide, acetic acid and butanol), but in this case the phenomenon masks phase transition from amorphous to anatase phase. Finally, an endothermic peak without any weight loss and probably associated with the anatase to rutile

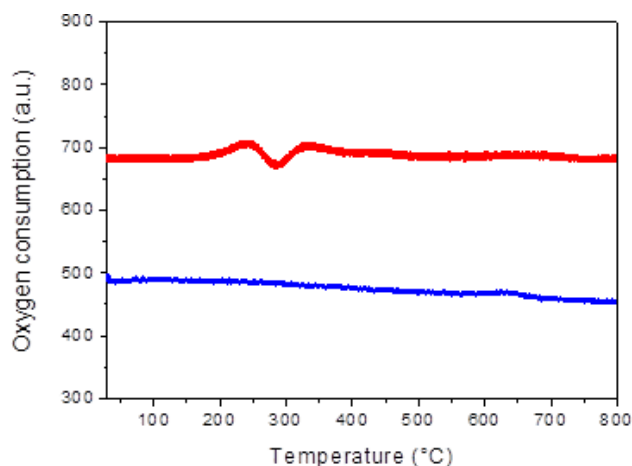


Figure 3. TPO profiles of T (blue curve) and commercial (red curve) samples.

phase transition,^[44] is observed in the DTA curve at high temperature (600–800 °C). The TG/DTA results indicate that the calcination temperature is probably too high and that no residual carbon species are reasonably preserved at 350 °C. However, it is not possible to reduce calcination temperature because it would have a negative effect on crystallinity. To confirm such hypothesis TPO analyses have been carried out on the T catalyst and on KRONOS 7000 sample. Two weak peaks due to oxygen consumption by two different carbonaceous species are observed in the TPO spectrum of commercial titania (red curve). On the contrary, no oxygen consumption has been observed on the T sample (blue curve), indicating that no carbon species are retained, in agreement with TG/DTA findings. Moreover, this feature has been also confirmed by the elemental analyses reported in table 1. Therefore, the adopted

Table 1. Surface areas of all samples and elemental analyses results (C and N amount) contrasted with synthesis parameters				
Sample	Chitosan/TiO ₂ w/w	Surface area m ² /g	C wt%	N wt%
T	-	134	-	-
Ch _{0,2} T	0,2	130	1,01	0,27
Ch _{0,4} T	0,4	130	3,44	1,06
Kronos 7000	-	289	0,86	

synthetic procedure did not guarantee the presence of any trace of carbon to remain in the photocatalyst, which seems to be a crucial feature for efficient catalysts in NO oxidation under visible light.

Chitosan effect on the photocatalysts

In order to enhance the titania photocatalytic performances under visible light, different amounts of chitosan, i.e. 0,2 and 0,4 w/w chitosan to titania ratios, were introduced during the synthetic procedure. Additional TG/DTA analyses were per-

formed to assure the eventual retention of some organic species, containing both N and C, on the calcined samples and, at the same time, try to verify the occurrence of the titania phase transition to anatase. The TG/DTA analyses of the as prepared Ch_{0,2}T (section a) and Ch_{0,4}T (section b) samples before calcination are shown in Figure 4. Two different

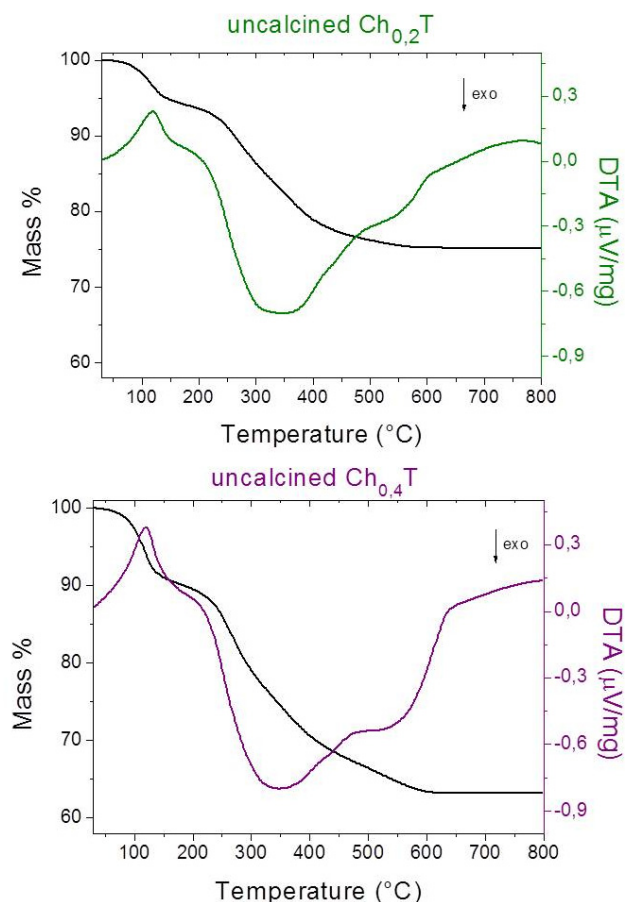


Figure 4. TG/DTA analysis of the as prepared Ch_{0,2}T (section a) and Ch_{0,4}T (section b) samples before calcination.

exothermic processes occurred by increasing the temperature: the former takes place between 300 °C and 450 °C, similarly to the chitosan-free sample (see Figure 2). Afterwards, the latter exothermic phenomenon is observed in the 450 °C - 600 °C range, causing a further weight loss. This second peak is more intense and the weight loss is greater for Ch_{0,4}T than for Ch_{0,2}T. Moreover, it was not observed in the case of the T sample during the TG/DTA analysis (see Figure 2) and it can be definitely ascribed to the chitosan oxidation. Previous TGA results revealed that the thermal decomposition of pure chitosan occurs into two stages, the former one is attributed to the loss of water in the 30–150 °C temperature range, whereas the latter one is due to the (thermal and oxidative) degradation of chitosan polymer chains by vaporization and elimination of volatile products (such as carboxylic and amino groups, respectively).^[45] Also in these cases, due to the occurrence of oxidation of the organic species, the phase transition from

amorphous titania to anatase is not clearly observable. The TG/TGA data clearly indicate that the calcination at 350 °C allowed to carbon and/or nitrogen to remain into the sample, as confirmed by the TPO analyses carried out on the same samples after calcination and reported in Figure 5. Indeed,

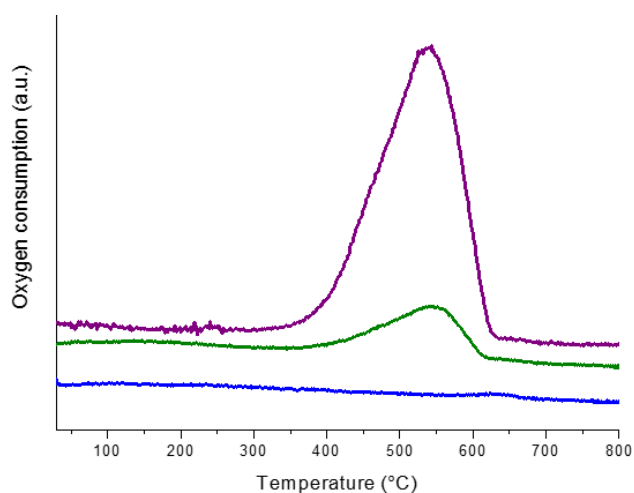


Figure 5. TPO spectra related to T (blue curve), $\text{Ch}_{0.2}\text{T}$ (green curve) and $\text{Ch}_{0.4}\text{T}$ (violet curve) samples.

differently from the T sample (blue curve), a peak related to oxygen consumption has been observed for both $\text{Ch}_{0.4}\text{T}$ (violet curve) and $\text{Ch}_{0.2}\text{T}$ (green curve) photocatalysts. Moreover, as indicated previously, the intensity of this peak increases with the increase of chitosan content in the sample.

TPO measurements are in agreement with the TG/DTA analyses, pointing out that some carbon and/or nitrogen species still remain in both $\text{Ch}_{0.2}\text{T}$ and $\text{Ch}_{0.4}\text{T}$ samples after the calcination process. As a matter of fact, a single peak of oxygen consumption between 400 °C and 600 °C is observed for both samples and such feature indicates that the oxidation of similar organic species deriving from chitosan took place. This signal is more intense in $\text{Ch}_{0.4}\text{T}$, in accordance with its higher amount of dopant. TG/DTA and TPO analyses put in evidence that organic species from a sustainable and environmentally friendly source such as chitosan are allowed to remain in the photocatalyst by using a single-step synthetic procedure. It is well known that even low amount of dopants considerably increases titania photoactivity.^[40]

Indeed, the catalytic tests shown in Figure 6 show that the presence of chitosan within the synthetic process increases the effectiveness displayed by the T sample in NO photooxidation from 32 % to 50% for $\text{Ch}_{0.2}\text{T}$ (green cylinder) and to 47% for $\text{Ch}_{0.4}\text{T}$ (violet cylinder).

Therefore, the one-pot synthesis procedure to insert chitosan effectively improves the photocatalytic performance of TiO_2 . However, co-doped titania samples are still less efficient than the commercial reference material (red cylinder). Apparently, the performance seems not dependent from the amount of chitosan inserted. Elemental analyses data (reported in Table 2) confirm the presence of nitrogen and carbon in both

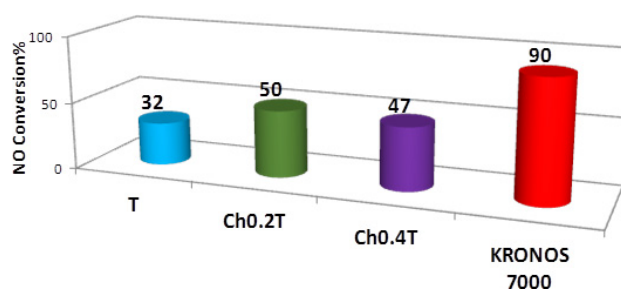


Figure 6. NO conversion obtained for the T, $\text{Ch}_{0.2}\text{T}$ and $\text{Ch}_{0.4}\text{T}$ samples compared with the commercial catalyst.

Table 2. Surface areas of all samples and elemental analyses results (C and N amount) contrasted with synthesis parameters.

Sample	Chitosan/ TiO_2 w/w	Acac/ $\text{Ti}(\text{O}-\text{Bu})_4$	Surface area m^2/g	C wt%	N wt%
$\text{A}_{0.7}\text{T}$	-	0.7	128	0.57	-
$\text{Ch}_{0.2}\text{A}_{0.7}$	0.2	0.7	150	0.57	0.20
T	-	-	-	-	-
$\text{Ch}_{0.4}$	0.4	0.7	151	1.52	1.06
$\text{A}_{0.7}\text{T}$	-	-	-	-	-

promoted samples. In particular, the content of C and N dopants is proportional to the initial amount of chitosan inserted during the synthesis. Moreover, the residual carbon in the lab made samples is higher (especially in the case of the $\text{Ch}_{0.4}\text{T}$ system) than that present in the commercial photocatalyst.

Therefore, it can be supposed that, on one hand, carbon and nitrogen relatively high amount promotes photoactivity, but, on the other, promoters cover catalytic sites without a big improvement in photocatalytic performances.

However, the effect of the dopant on the properties of titania has been further investigated in order to explain the observed increase in photoactivity of the $\text{Ch}_{0.2}\text{T}$ and $\text{Ch}_{0.4}\text{T}$ samples. The UV-Vis-NIR spectra of both T (blue curve) and $\text{Ch}_{0.2}\text{T}$ (green curve) samples are reported in section b of Figure 7. Generally, the addition of chitosan seems to have no influence the electronic properties of titania since any change in oxide band gap has been observed (3.2 eV for both samples). However, a broad and complex absorption band in the 27000-8000 cm^{-1} range is evident when the synthesis is carried out in the presence of chitosan (see section c of the same figure). Moreover, the two photocatalysts display different colors, since the T sample is white, whereas the sample modified by chitosan is light grey (section a of Figure 7).^[46] Thus, the broad absorption can be related to the presence of residual molecular fragments coming from the decomposition of chitosan that occurred during the calcination at 350 °C, according to TPO measurements.

In addition, FTIR experiments were carried out on the samples outgassed at increasing temperature in order to remove water from the surface and to investigate the nature of residual surface species coming from chitosan, whose presence

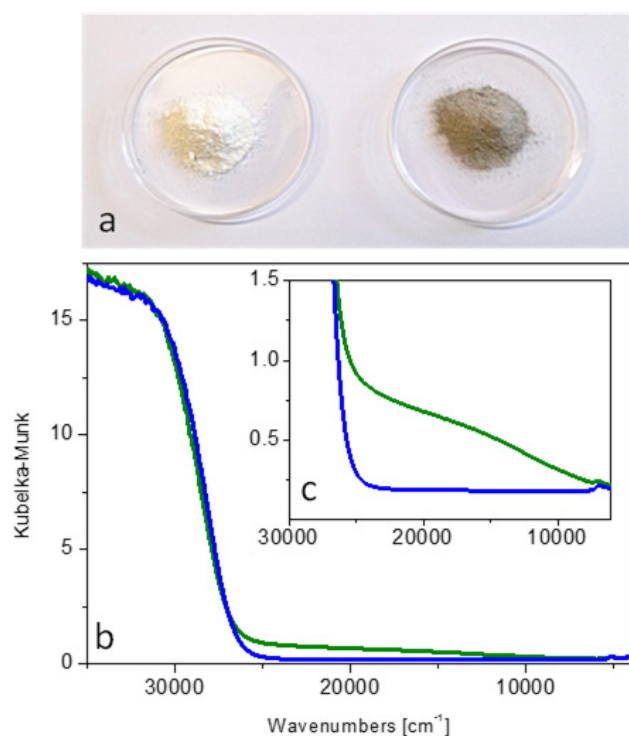


Figure 7. Diffuse Reflectance UV-Vis spectra related to T (blue curve) and $\text{Ch}_{0.2}\text{T}$ (green curve) samples.

has been put in evidence in Figure 8. The FTIR absorbance spectra normalised with respect to the weight of the pellets of T (blue curves) and $\text{Ch}_{0.2}\text{T}$ (green curves) samples are reported in Figure 9.

The spectra have been collected under outgassing at increasing temperature. Upon increasing the temperature up to $150\text{ }^{\circ}\text{C}$, a decrease in intensity of the broad absorption at about 3200 cm^{-1} as well as of the peak at 1620 cm^{-1} , due to the presence of water, is observed. The addition of chitosan produced almost negligible changes in the spectra. However, according to thermogravimetric and UV-Vis findings, weak bands at 1594 , 1398 and 1187 cm^{-1} are observed on the surface photocatalyst outgassed at $150\text{ }^{\circ}\text{C}$, as shown in Figure 9, green curve. The bands at 1594 and 1187 cm^{-1} can be tentatively assigned to the sym and asym stretching modes of residual $\text{C}=\text{O}$ fragments, respectively.^[45] The component at 1398 cm^{-1} could be possibly related to the symmetric deformation mode of CH_3 group.^[47] However, no absorption due to nitrogen species on the catalytic surface has been detected, indicating that the observed increase in photoactivity is due to the sole presence of one of dopant. Summarising, the FTIR results revealed that nitrogen species do not interact with titania on the photocatalytic surface: this means that chitosan capacity to increase titania photoactivity under visible light is not fully exploited.

Moreover, all samples have been proven to have the same anatase crystal phase (data not shown) and also similar surface area values ($\sim 130\text{ m}^2/\text{g}$) as reported in Table 2. DR UV-Vis NIR and FTIR results along with the very high surface area of Kronos 7000 ($289\text{ m}^2/\text{g}$, Table 2) can be at the origin of the different

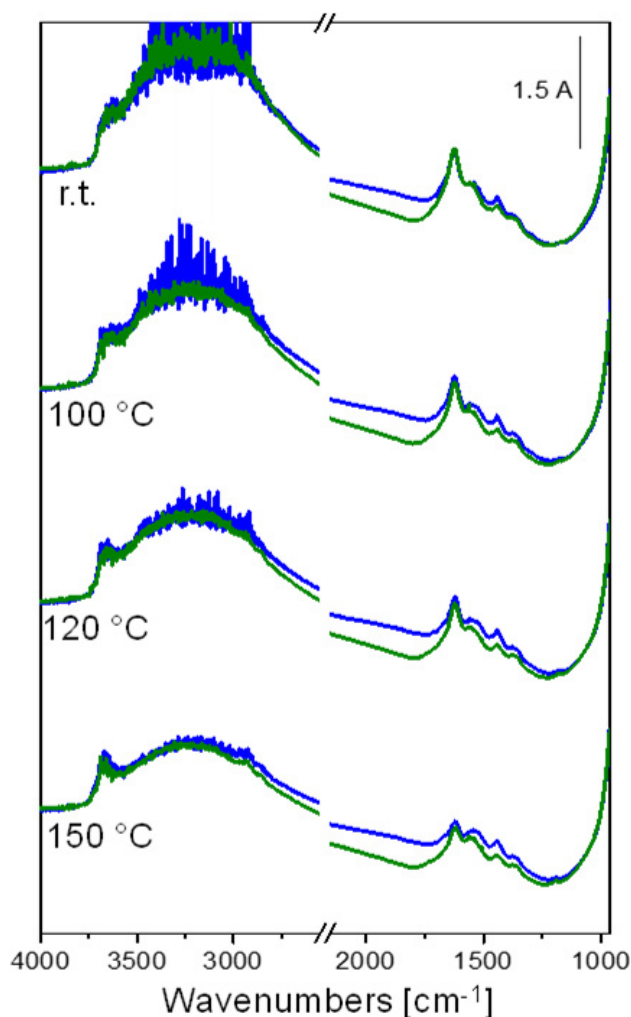


Figure 8. FTIR absorbance spectra normalised with respect to the weight of the pellets of T (blue curves) and $\text{Ch}_{0.2}\text{T}$ (green curves) samples under outgassing at increasing temperature.

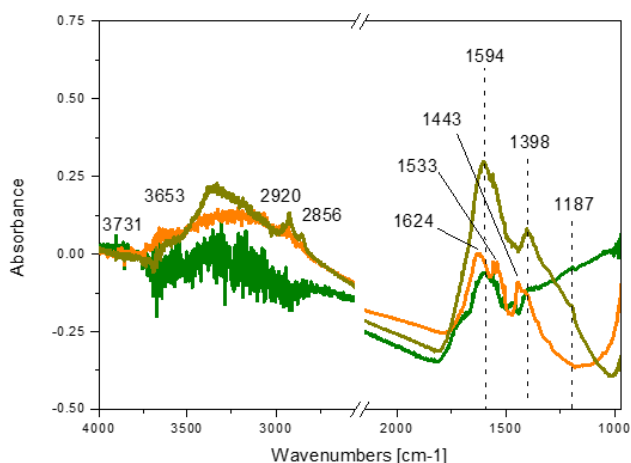


Figure 9. FTIR difference spectra of $\text{Ch}_{0.2}\text{T}$ (green curve), $\text{Ch}_{0.2}\text{A}_{0.7}\text{T}$ (orange curve) and $\text{Ch}_{0.4}\text{A}_{0.7}\text{T}$ (dark yellow curve) under outgassing at $150\text{ }^{\circ}\text{C}$. The spectrum of T collected at the same temperature was used as background for $\text{Ch}_{0.2}\text{T}$, the spectrum of $\text{A}_{0.7}\text{T}$ was subtracted to $\text{Ch}_{0.2}\text{A}_{0.7}\text{T}$ and $\text{Ch}_{0.4}\text{A}_{0.7}\text{T}$.

catalytic behaviour: the chitosan assisted synthesis has proven to be effective to promote TiO_2 photoactivity, but needs to be further optimised. In particular, the procedure has to be revised to enhance the specific surface area of the obtained materials and to enforce the effect of chitosan, by improving the interaction between the polymer and the oxide.

Influence of the addition of acetylacetone

It is well known that acetylacetone is a chelating molecule that is able to interact with titanium alkoxides, thus retarding the hydrolysis and condensation reactions involved in the sol-gel process.^[48] In such frame, it can be supposed that a more effective interaction between the chitosan molecule and the titania precursor occurs in the presence of acetylacetone. As a consequence, the specific surface area of titania might result enhanced^[49] and a positive change in the promoting effect of the dopants would be expected. Therefore, acetylacetone has been added in the synthetic process with the aim of obtaining samples with increased photocatalytic activity. On the basis of a previous work,^[50] the selected acac/Ti molar ratio is 0,7. Three additional samples with the same acac/Ti molar ratio and containing different amounts of chitosan have been prepared. The samples are labelled as $\text{A}_{0,7}\text{T}$, $\text{Ch}_{0,2}\text{A}_{0,7}\text{T}$ and $\text{Ch}_{0,4}\text{A}_{0,7}\text{T}$. N_2 Physisorption analyses were carried out to evaluate the effect of acetylacetone on the final surface area of the titania sample. The addition of the sole acetylacetone to the T sample does not change the surface area significantly (see also Table 1), nor crystal phase, however the co-presence of acetylacetone and chitosan has an effect. In particular, independently from the amount of chitosan, the presence of acetylacetone enhanced the surface area from $130 \text{ m}^2/\text{g}$ to $150 \text{ m}^2/\text{g}$ (see Table 2).

Moreover, TG/DTA analyses were performed on both as prepared $\text{Ch}_{0,2}\text{A}_{0,7}\text{T}$ (section a) and $\text{Ch}_{0,4}\text{A}_{0,7}\text{T}$ samples (Figure 10). Similarly to what previously observed, organic fragments from chitosan remain on the samples in which acetylacetone has been added during synthesis. The thermogravimetric profiles reveal that exothermic processes that are linked to weigh loss occur far above $350 \text{ }^\circ\text{C}$. However, if compared to the samples without acetylacetone and given the same amounts of chitosan (see Figure 4), the second exothermic peak related to $\text{Ch}_{0,2}\text{A}_{0,7}\text{T}$ is slightly shifted to lower temperature, being the maximum centred between $450 \text{ }^\circ\text{C}$ and $500 \text{ }^\circ\text{C}$ (instead of $550 \text{ }^\circ\text{C}$). This phenomenon is not noticeable in the case of $\text{Ch}_{0,4}\text{A}_{0,7}\text{T}$. Such feature might be a first indication that the addition of acetylacetone induces a modification of the chitosan-derived organic species present in the photocatalysts.

These samples have been then tested in the NO photocatalytic oxidation and the results are reported in Figure 10. First of all, the chitosan-free sample T (blue cylinder vs pink cylinder) shows almost the same photocatalytic behaviour when prepared either in the presence or in the absence of acetylacetone ($32 \text{ } \%$ vs $30 \text{ } \%$ NO conversion), indicating that the addition of acetylacetone has no influence on the photocatalytic activity. The effect of the addition of acetylacetone on the photocatalytic activity is also negligible in the case of $\text{Ch}_{0,4}\text{T}$ (violet cylinder) and $\text{Ch}_{0,4}\text{A}_{0,7}\text{T}$ (dark yellow cylinder). Carbon

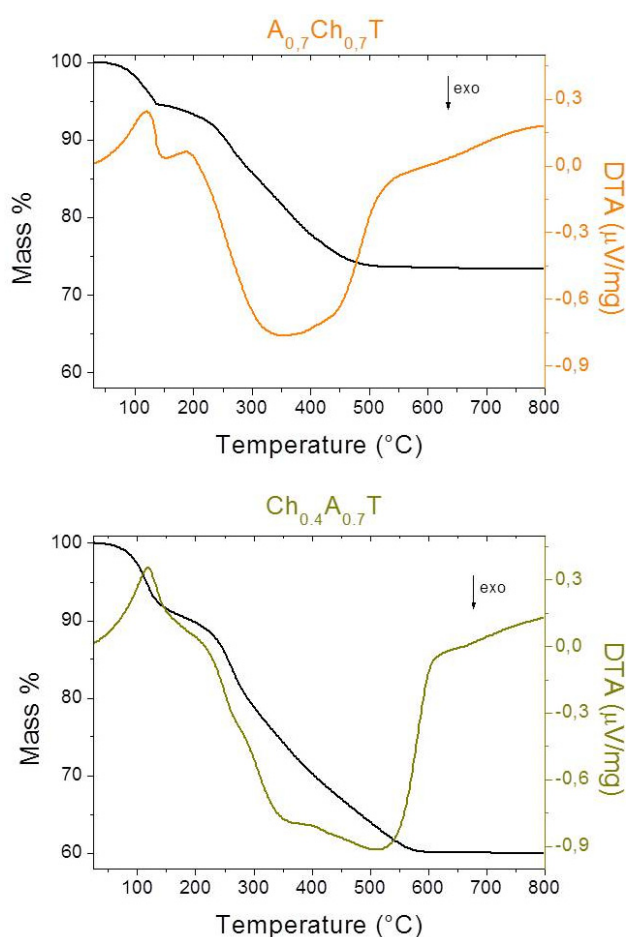


Figure 10. TG/DTA analyses of as prepared $\text{Ch}_{0,2}\text{A}_{0,7}\text{T}$ (a) and $\text{Ch}_{0,4}\text{A}_{0,7}\text{T}$ (b).

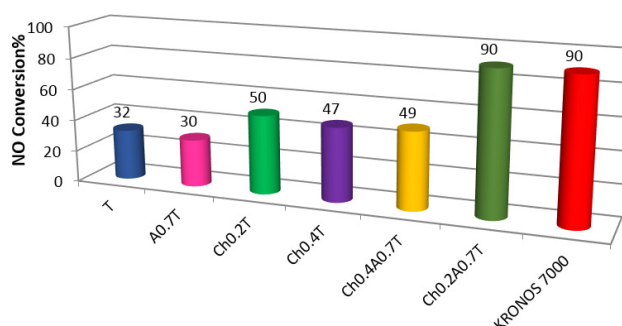


Figure 11. Photocatalytic activity result for all the synthesized sample and for KRONOS 7000.

and nitrogen amount in the sample prepared in presence of acetylacetone is roughly half of the same sample without chelating agent, but it is probable that carbon and nitrogen amount is still not low enough to make the surface sites completely available (see Table 2). Differently, the addition of acetylacetone in the single-step synthetic process almost doubles the photoactivity of the sample with a chitosan/ titania weight ratio of 0,2: $\text{Ch}_{0,2}\text{T}$ (green cylinder) shows $50 \text{ } \%$ NO conversion, whereas $\text{Ch}_{0,2}\text{A}_{0,7}\text{T}$ (orange cylinder) displays $90 \text{ } \%$

NO conversion, which is the same value attained for the commercial photocatalyst (red cylinder).

Such tremendous increase in photoactivity cannot be exclusively ascribed to the increase in specific surface area: indeed the surface area of $\text{Ch}_{0.2}\text{A}_{0.7}\text{T}$ is $150\text{ m}^2/\text{g}$ vs $289\text{ m}^2/\text{g}$ of Kronos 7000. Moreover, $\text{Ch}_{0.2}\text{A}_{0.7}\text{T}$ and $\text{Ch}_{0.4}\text{A}_{0.7}\text{T}$ have the same surface area ($150\text{ m}^2/\text{g}$ and $151\text{ m}^2/\text{g}$, respectively). In addition, independently from the presence of chitosan or acetylacetone, all samples have been proven to have the same anatase crystal phase, as shown in Figure 12.

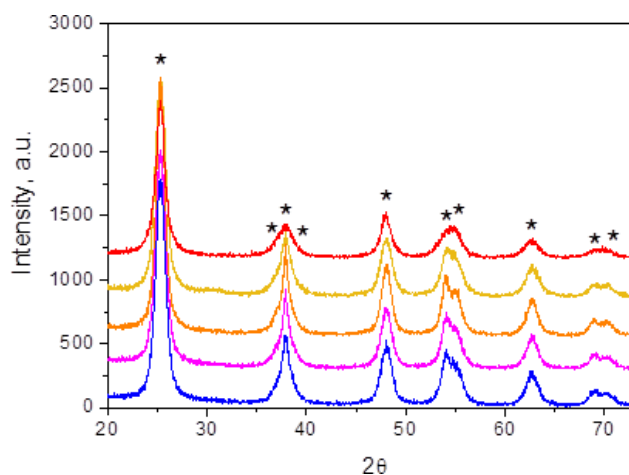


Figure 12. XRD patterns of T (blue curve), $\text{A}_{0.7}\text{T}$ (magenta curve), $\text{Ch}_{0.2}\text{A}_{0.7}\text{T}$ (orange curve) and $\text{Ch}_{0.4}\text{A}_{0.7}\text{T}$ (dark yellow curve) samples calcined at 350°C and of commercial Kronos 7000 (red curve).

The comparison with the XRD pattern related to Kronos 7000 (red pattern) reveals that the peaks appearing in the patterns related to the titania samples prepared in this work are generally more intense and narrower than those observed for the commercial sample. This feature is in agreement with the results of N_2 adsorption-desorption measurements reported in Table 2. Therefore, the huge increase in the photocatalytic activity can be ascribed to an enhanced interaction between the chitosan molecule and the titania precursor in the presence of acetylacetone, due to its retarding action on the titanium alkoxide hydrolysis during the one-pot synthesis. Elemental analyses were performed in order to have information on the C and N amounts in all the samples and the results are summarised in Table 2. According to the structure of polyglucoseamine, the C amount of is higher than the N amount in all chitosan-based materials. Moreover, given the same chitosan amount, the values found for C and N are lower in the presence of acetylacetone, i.e. as for C and N entries in Table 2: $\text{Ch}_{0.2}\text{T} > \text{Ch}_{0.2}\text{A}_{0.7}\text{T}$ and $\text{Ch}_{0.4}\text{T} > \text{Ch}_{0.4}\text{A}_{0.7}\text{T}$. In addition, according to Table 2, the catalyst with the best catalytic performance ($\text{Ch}_{0.2}\text{A}_{0.7}\text{T}$) is the one having the lowest amount of dopants. These experimental data point out that to achieve photoactivity is fundamental to have the best synergy between the total amount of carbon and nitrogen and the optimal interaction

between dopants and the titania oxides. This last finding needs to be precisely investigated.

3.4 Nature of the interaction among the dopants and the oxide

Diffuse reflectance UV-Vis spectra of $\text{A}_{0.7}\text{T}$ (magenta curve), $\text{Ch}_{0.2}\text{A}_{0.7}\text{T}$ (orange curve) and $\text{Ch}_{0.4}\text{A}_{0.7}\text{T}$ (dark yellow curve) are reported in Figure 13. The spectrum of $\text{Ch}_{0.2}\text{T}$ is also reported

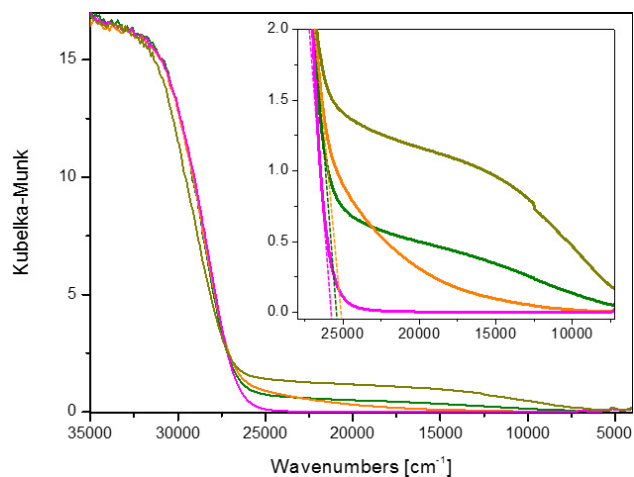


Figure 13. DR UV-Vis spectra of $\text{A}_{0.7}\text{T}$ (magenta curve), $\text{Ch}_{0.2}\text{A}_{0.7}\text{T}$ (orange curve), $\text{Ch}_{0.4}\text{A}_{0.7}\text{T}$ (dark yellow curve) and $\text{Ch}_{0.2}\text{T}$ (green curve).

for comparison (green curve). The bare $\text{A}_{0.7}\text{T}$ sample does not provide any absorption in the visible region and its value of band-gap is typical for blank anatase titania (magenta curve). Differently, $\text{Ch}_{0.2}\text{A}_{0.7}\text{T}$ (orange curve) and $\text{Ch}_{0.4}\text{A}_{0.7}\text{T}$ (dark yellow curve) show absorption in the visible region. However, if comparing the spectra of $\text{Ch}_{0.2}\text{A}_{0.7}\text{T}$ and $\text{Ch}_{0.4}\text{A}_{0.7}\text{T}$, such absorptions do not look similar as for both shape and intensity.

Moreover, besides having the highest intensity due to the highest amount of chitosan, (green curve) the spectrum of $\text{Ch}_{0.4}\text{A}_{0.7}\text{T}$ displays very similar shape as that related to the $\text{Ch}_{0.2}\text{T}$ sample. These features are an indication that different processes occurred during synthesis and calcination of the two $\text{Ch}_{0.2}\text{A}_{0.7}\text{T}$ and $\text{Ch}_{0.4}\text{A}_{0.7}\text{T}$ photocatalysts giving rise to different electronic properties. Furthermore, the occurrence of comparable phenomena in the case of $\text{Ch}_{0.4}\text{A}_{0.7}\text{T}$ and $\text{Ch}_{0.2}\text{T}$ samples can be hypothesised, given the very similar UV-Vis spectra profiles. FTIR experiments at increasing temperature have been carried out with the aim to investigate the nature of the residual surface species on the $\text{Ch}_{0.2}\text{A}_{0.7}\text{T}$ and $\text{Ch}_{0.4}\text{A}_{0.7}\text{T}$ samples. The FTIR absorbance spectra normalised with respect to the weight of the pellets of bare $\text{A}_{0.7}\text{T}$ (magenta curves), $\text{Ch}_{0.2}\text{A}_{0.7}\text{T}$ (orange curves) and $\text{Ch}_{0.4}\text{A}_{0.7}\text{T}$ (dark yellow curves) are shown in Figure 14.

Similarly to what previously observed for T and $\text{Ch}_{0.2}\text{T}$ (Figure 8, blue and green curves, respectively) the increase of the temperature up to 150°C , produces a decrease in intensity

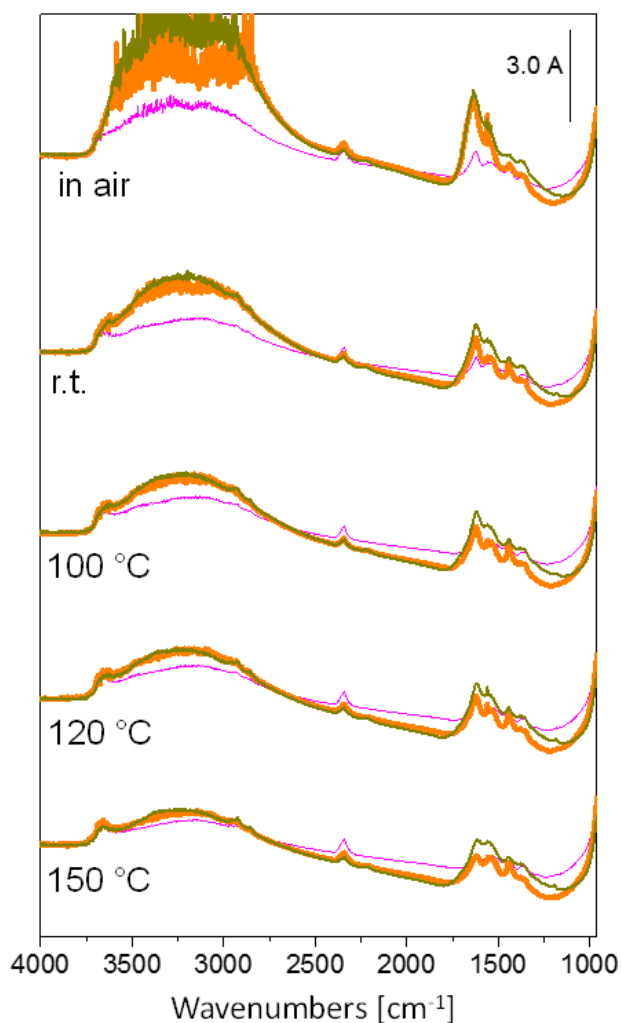


Figure 14. FTIR absorbance spectra normalised with respect to the weight of the pellets of $A_{0.7}T$ (magenta curves), $Ch_{0.2}A_{0.7}T$ (orange curves) and $Ch_{0.4}A_{0.7}T$ (dark yellow curves) samples in air and under outgassing at increasing temperature.

of the bands related to the presence of water. Unexpectedly, in this case the addition of chitosan induced a modification in the spectra at frequencies lower than 2500 cm^{-1} , due to the erosion of an electronic absorption (orange and dark yellow curves) and the entity of the modification is more evident on increasing the temperature up to $150\text{ }^{\circ}\text{C}$. Such electronic absorption is related to free electrons in the conduction band of titania (magenta curve). These electrons are trapped by the presence of residual chitosan fragments causing the erosion of the absorption above described. This phenomenon is more pronounced for $Ch_{0.2}A_{0.7}T$ (orange curves) than for $Ch_{0.4}A_{0.7}T$ (dark yellow curves). Moreover, quite strong bands at 1594 and 1187 cm^{-1} due to the sym and asym stretching modes of residual carboxylic fragments^[45] accompanied by bands 1398 , 2856 and 2920 cm^{-1} corresponding to the bending mode of CH_3 group and possibly to the stretching mode of CH_3 and CH_2 or CH units^[47,51] have been detected on the $A_{0.7}Ch_{0.4}T$ photocatalyst outgassed at $150\text{ }^{\circ}\text{C}$, as shown in Figure 14, dark yellow

curve. On the contrary, beside the absorption bands at 1398 , 2856 and 2920 cm^{-1} already assigned to the vibrations of residual CH_x groups, new components at 1443 , 1533 , 1624 , 3653 and 3731 cm^{-1} are observed for $A_{0.7}Ch_{0.2}T$ (Figure 14, orange curve). The band at 1443 cm^{-1} can be tentatively assigned to the coupling of C-N axial stretching and N-H angular deformation.^[52] The bands at 1533 and 1624 cm^{-1} could be possibly related to the bending modes of unconsumed ammonium units^[49] and the small peaks observed at 3653 and 3731 cm^{-1} can be due to the stretching of OH groups on titania^[53] and to OH belonging to species remaining at the surface, respectively. In agreement with the diffuse reflectance UV-Vis findings, all the above FTIR features indicate that, differently from the case of the $Ch_{0.2}T$ and $A_{0.7}Ch_{0.4}T$ samples, N-containing species are located at the surface of the $A_{0.7}Ch_{0.2}T$ photocatalyst, further confirming the occurrence of a distinct interaction phenomenon between titania and chitosan during synthesis and calcination at $350\text{ }^{\circ}\text{C}$. It was reported that the weight loss of pure chitosan involved the release of H_2O , NH_3 , CO , CO_2 and CH_3COOH and that the release of ammonia started at lower temperatures than the other species, reaching the highest rate at $325\text{ }^{\circ}\text{C}$ and suggesting that the formation of NH_3 needs a low activation energy.^[49] It can be proposed that the loss of ammonia is hindered for $A_{0.7}Ch_{0.2}T$, as also supported by the smaller weight loss observed during TG/DTA analysis (Figure 10) and hence guaranteeing a more effective modification of titania by both C and N dopants. This means that in this sample nitrogen species, as long as carbon species, are present on the photocatalytic surface, whereas in the other samples only carbonaceous species are detected. It is worth noting that the FTIR measurements gave also evidence of a modification of the electronic properties of titania induced by the presence of residual C and N species coming from the decomposition of chitosan during the calcination at $350\text{ }^{\circ}\text{C}$.

Further FTIR experiments of CO adsorbed at low temperature on the as prepared $A_{0.7}T$, $Ch_{0.2}A_{0.7}T$ and $Ch_{0.4}A_{0.7}T$ samples were performed and the results are reported in Figure 15 in the carbonylic region.

Upon the inlet of 15 mbar CO at $-180\text{ }^{\circ}\text{C}$, bands at 2178 cm^{-1} , due to CO adsorbed Ti^{4+} sites on regular (0 1 0) and (0 0 1) faces,^[53] and at 2150 cm^{-1} , assigned to CO molecules hydrogen bonded to OH groups,^[53] are produced. The intensity of these bands is maximum in the case of $A_{0.7}T$, indicating that the surface is more free than that of the chitosan-containing samples. Moreover by decreasing the CO pressure, the band at 2176 cm^{-1} , due to Ti^{4+} sites slightly red shifts due to dipole-dipole interactions occurring only on $A_{0.7}T$ and therefore demonstrating the presence of isolated Ti^{4+} sites on the other chitosan-containing samples. Finally, the absorption related to CO in interaction with OH groups appears broader with the increase in chitosan content, putting in evidence an enhance in heterogeneity of the sites at the surface. Therefore, beside the promotion of the specific surface area of titania, the addition of acetylacetone effectively modifies the surface as well as the electronic properties of the C, N-doped titania photocatalyst. Indeed, the interaction between the dopant species and the titanium dioxide is improved in the presence of acetylacetone.

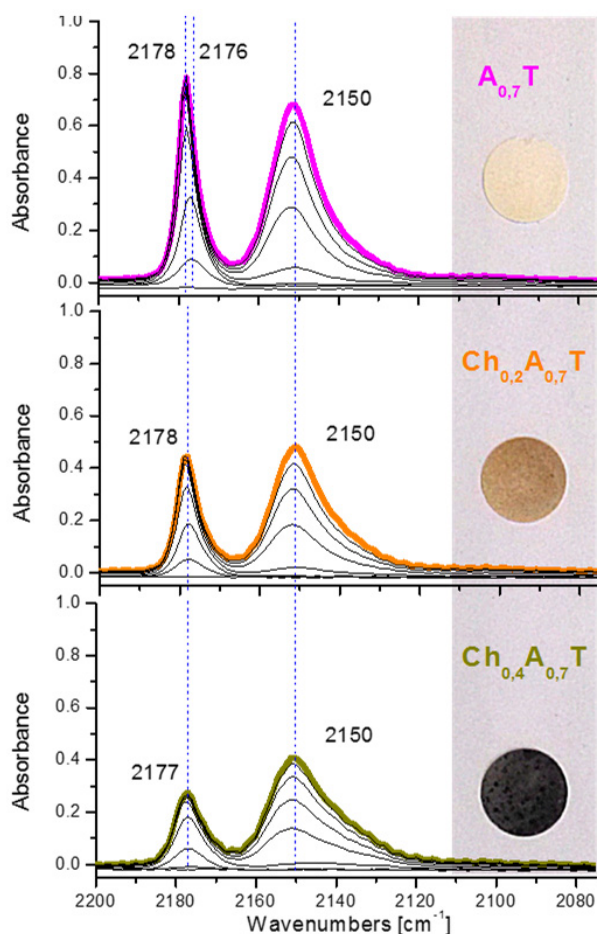


Figure 15. FTIR difference spectra collected upon the inlet of 15 mbar CO at $-190\text{ }^{\circ}\text{C}$ on $\text{A}_{0.7}\text{T}$ (magenta curve), $\text{Ch}_{0.2}\text{A}_{0.7}\text{T}$ (orange curve) and $\text{Ch}_{0.4}\text{A}_{0.7}\text{T}$ (dark yellow curve), at decreasing CO pressures and under outgassing at the same temperature (black curves). Insets: images of the pellets of the samples.

Upon calcination at $350\text{ }^{\circ}\text{C}$, residual $\text{C}_x\text{N}_y\text{H}_z$ species are present at the titania surface. Such species induce an electronic modification of the oxide by trapping electrons of the conduction band and favoring the e^- -hole separation. It has been reported that in any C-doped titania C 2p and O 2p mixing has never been observed, but only discrete mid-gap states have been detected.^[54,55] Moreover, oxygen excess in calcination favors interstitial N-doping.^[12] A slight decrease of the band gap is also observed (as shown in the inset of Figure 13).

Conclusions

Chitosan, a widely available natural product, has proven to be an effective and sustainable source of carbon and nitrogen for titania promotion in order to increase photoactivity in NO oxidation under visible light. This innovative synthetic approach allows the simultaneous introduction of carbon and nitrogen during the preparation of the titania photocatalysts using a single source of promoters. A careful tuning of the synthetic

parameters allowed to formulate a photocatalyst whose efficiency is comparable to that provided by reference commercial titania that is specifically designed to be photoactive under visible light. It is fundamental to highlight that this approach presents significant advantages if compared to that employed for the preparation of the best commercial catalyst that is synthesized by a two steps procedure by using acid succinic and/or pentaerythritol as C source. On the contrary, the synthetic procedure optimized in this work, is a one-step method: fast from the viewpoint of the synthesis procedure, cheap, reproducible and sustainable. Indeed, a natural, biodegradable and biocompatible polymer such as chitosan increases the visible light absorption and modifies titania electronic properties. Such procedure represents therefore an effective and industrially attractive way to obtain a highly active titania photocatalyst under visible light for a real application in coating, paints and green building industry.

Experimental Section

Photocatalyst synthesis

The following reagents were used as received: titanium(IV) tetrabutoxide $\text{Ti}(\text{OC}_4\text{H}_9)_4$ (97 %, Sigma Aldrich), acetylacetone (99,5 %, Sigma Aldrich), butanol (99 %, Sigma Aldrich), acetic acid (99,9%, Sigma Aldrich) and chitosan (medium molecular weight, Sigma Aldrich). As a standard reference material, KRONOS VLP 7000 has been purchased by KRONOS INC. The synthetic procedure reported by Kavitha et al^[55] has been modified according to the purposes of this work. For the sake of clarity, the main steps of the one-pot synthesis are shown in Figure 16.

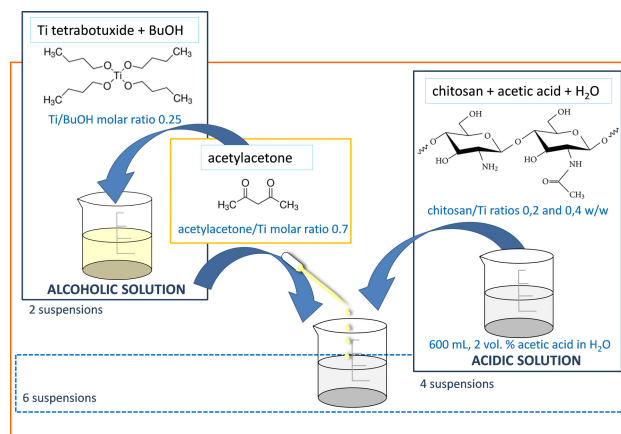


Figure 16. Main steps of the one-pot synthesis procedure.

Titanium tetrabutoxide has been solved separately in butanol (BuOH) maintaining a molar ratio Ti:BuOH of 1:4. An aliquot of such solution was added with acetylacetone in order to obtain an acetylacetone/titanium molar ratio equal to 0,7. In another beaker, different amounts of chitosan have been

solved in 600 mL of 2 vol. % acetic acid aqueous solution. Afterwards, the alcoholic solution containing the Ti precursor has been added dropwise to the acidic chitosan solution. Two chitosan to titania ratios, namely 0,2 and 0,4 w/w, have been prepared.

Six different suspensions have been obtained following the above procedure. Then each mixture has been aged in a sealed Teflon vessel at 90 °C and autogenous pressure for 40 hours. The samples have been dried overnight at 90 °C and finally calcined at 350 °C under a 50 mL·min⁻¹ air flow for 3 h.

The obtained materials are summarised in Table 3, where the Chitosan/TiO₂ and Acetylaceton/Ti(OBu)₄ molar ratios are

Table 3. List of the samples and employed synthetic parameters		
Sample	Chitosan/TiO ₂ w/w	Acac/Ti(OBu) ₄ mol/mol
T	-	-
A _{0,7} T	-	0,7
Ch _{0,2} T	0,2	-
Ch _{0,4} T	0,4	-
Ch _{0,2} A _{0,7} T	0,2	0,7
Ch _{0,4} A _{0,7} T	0,4	0,7

also reported. The samples have been labelled Chx(A)T where Ch stands for chitosan, x for chitosan/titania weight ratio A stands for acetylaceton and T for titanium dioxide calcined at 350 °C.

Characterization of the photocatalysts

Thermal analyses (TG/DTA) were performed on a NETZSCH STA 409 PC/PG instrument in air flux (20 mL/min) using a temperature rate set at 5 °C/min in the 25–800 °C temperature range.

X-Ray Diffraction (XRD) patterns of the samples were collected employing a Bruker D8 Advance powder diffractometer with a sealed X-ray tube (copper anode; operating conditions, 40 kV and 40 mA) and a Si(Li) solid state detector (Sol-X) set to discriminate the Cu K α radiation. Apertures of divergence, receiving and detector slits were 2.0 mm, 2.0 mm, and 0.2 mm respectively. Data scans were performed in the 2 θ range 5–75° with 0.02° step size and counting times of 3 s/step. Quantitative phase analysis and crystallite size determination were performed by the Rietveld method as implemented in the TOPAS v.4 program (Bruker AXS) using the fundamental parameters approach for line-profile fitting. The determination of crystallite size was accomplished by the Double-Voigt approach and calculated as volume-weighted mean column heights based on integral breadths of peaks.

N₂ adsorption-desorption isotherms at -196 °C were performed using a MICROMERITICS ASAP 2000 analyser in order to measure specific surface areas and pore volumes. Prior to N₂ physisorption experiments, all samples were outgassed at 200 °C for 2 hours. Mesopore volume was measured as the adsorbed amount of N₂ after capillary condensation. Surface area was calculated using the standard Brunauer, Emmett and

Teller (BET)^[56] equation method and pore size distribution was elaborated using the BJH method applied to the isotherms desorption branch.^[57]

Temperature programmed oxidation (TPO) experiments have been carried out in a lab-made equipment: samples (50 mg) have been heated at 10 °C/min from 25 °C to 700 °C in a 5% O₂/He oxidative mixture (40 mL/min STP). The effluent gases have been analysed by a Gow-Mac TCD detector using a basic trap with soda lime to adsorb CO₂ and a magnesium perchlorate trap to stop H₂O.

For diffuse reflectance UV–Vis–NIR analysis, powders were placed in a quartz cell, allowing treatments in controlled atmosphere and temperature, but spectra recording only at room temperature (r.t.). Diffuse reflectance UV–Vis–NIR spectra were run at r.t. on a Varian Cary 5000 spectrophotometer, working in the 50000–4000 cm⁻¹ range. UV–Vis–NIR spectra of the as prepared samples are reported in the Kubelka-Munk function $[f(R_{\infty}) = (1 - R_{\infty})^2 / 2R_{\infty}]$; R ∞ = reflectance of an “infinitely thick” layer of the sample.

Transmission FTIR measurements have been performed on the samples in self-supporting pellets introduced in cells allowing thermal treatments in controlled atmospheres and spectrum scanning at controlled temperatures (from -196 °C to 150 °C). The FTIR spectra were taken on a Perkin Elmer 2000 spectrometer (equipped with a cryogenic MCT detector). As for the analyses at increasing temperature, each sample was introduced in an AABSPEC 2000 cell allowing to run the spectra in situ in controlled atmosphere and temperature. The samples were outgassed from room temperature (r.t.) up to 150 °C. As for the measurements at low temperature, the samples were submitted to outgassing at r.t. for 1 hour in order to remove water, due to the exposition to air, and to avoid the modification of the residual coming from the decomposition of chitosan. Then the samples were cooled at -196 °C. All spectra were normalised with respect to the density of the pellets. As for the CO adsorption experiment, the spectrum of the sample before the inlet of CO was subtracted from each spectrum.

Elemental analyses were performed by the Microanalysis Laboratory of the Dept. of Chemical Sciences of the University of Padova with a Fison EA1108 CHNS Analyzer.

Photocatalytic tests

The evaluation of the photocatalytic activity in NO oxidation has been estimated using an experimental apparatus as previously reported.^[58] The reaction has been carried out in gas phase in a fixed-bed reactor at atmospheric pressure and room temperature by feeding a 1000 mL·min⁻¹ flow of NO/air mixture (NO concentration is 100 ppb). A typical experiment requires 50 mg of catalyst, that have been previously pressed, ground and sieved to 50–70 mesh (corresponding to 0.2–0.3 mm). The catalyst has been introduced into a microreactor with 2 mm internal diameter and irradiated with a visible lamp (fluorescent energy saver lamp, Philips WW 827,14W) which provides an irradiance of 7.5 W·m⁻².

Before starting the photooxidation reaction, the reactor was purged and saturated with pure air. NO concentration was

monitored in continuous and a typical profile of such concentration as a function time has been reported in Figure 17 as representative plot.^[59,60]

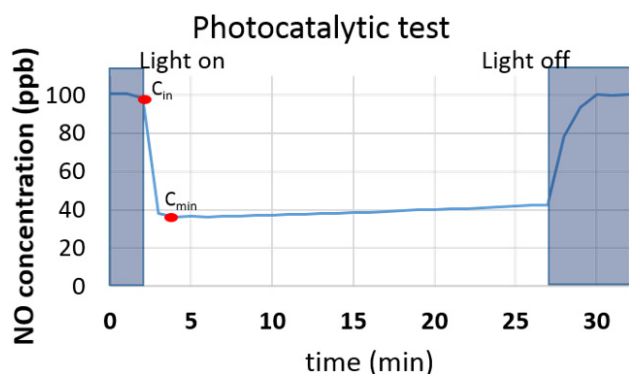


Figure 17. Typical NO concentration profile observed during the catalytic tests.

As it can be observed, NO concentration reaches a minimum value followed by a slow and continuous deactivation process after the adsorption of NO₂ on the catalytic active sites.^[58]

The catalytic efficiency is expressed in terms of conversion of NO, calculated with the following equation:^[61,62] conversion % = $(C_{in} - C_{min}) / C_{in} \times 100$ where C_{in} is the initial concentration of NO and C_{min} is the minimal concentration of NO. Catalytic results are reproducible and the catalytic conversion reported was determined as the average of three independent analyses. Based on the above considerations, the minimum value of the concentration of NO was considered as key parameter for the evaluation of the catalytic performances. A blank test was performed in the same reactor in the absence of irradiation: NO was weakly adsorbed on the titania surface, but no conversion was detected.

The photocatalytic results have been compared to those obtained with the commercial reference material.

Acknowledgements

The authors thank Tania Fantinel (Ca' Foscari University of Venice) and Giulia Braggaglia for the excellent technical assistance. For financial support, the authors acknowledge Regione Veneto and European Social Found (Project 2120/10/2121/2015).

Conflict of Interest

The authors declare no conflict of interest.

Keywords: Chitosan · C-N-doping · One-Pot · Photocatalysis · Titania

[1] M. R. Hoffmann, S. T. Martin, W. Choi, D. W. Bahnemann, *Chem. Rev.* **1995**, *95*, 69–96.

- [2] A. Folli, C. Pade, T. Baek Hansen, T. De Marco, D. E. Macphee, *Cem. Concr. Res.* **2012**, *42*, 539–548.
- [3] T. Ohno, K. Sarukawa, K. Tokieda, M. Matsumura, *J. Catal.* **2001**, *203*, 82–86.
- [4] S. Hackenberg, G. Friehs, K. Froelich, C. Ginzkey, C. Koehler, A. Scherzed, M. Urghartz, R. Hagen, N. Kleinsasser, *Toxicol. Lett.* **2010**, *195*, 9–14.
- [5] A. L. Linsebiegler, G. Lu, J. T. Yates, *Chem. Rev.* **1995**, *95*, 735–758.
- [6] A. Kubacka, M. Fernández-García, G. Colón, *Chem. Rev.* **2012**, *112*, 1555–1614.
- [7] K. M. Parida, B. Naik, *J. Colloid Interf. Sci.* **2009**, *333*, 269–276.
- [8] B. O'Regan, M. Grätzel, *Nature* **1991**, *353*, 737–740.
- [9] M. Grätzel, *Nature* **2001**, *414*, 338–344.
- [10] Y. Li, M. Guoa, S. Peng, G. Lu, S. Li, *Inter. J. Hydrogen Energy* **2009**, *34*, 5629–5636.
- [11] Y. Li, Y. Jiang, S. Peng, F. Jiang, *J. Hazard. Mater.* **2010**, *182*, 90–96
- [12] L. Gomathi Devi, R. Kavitha, *Applied Catalysis B: Environmental* **2013**, *140–141*, 559–587.
- [13] V. Trevisan, E. Ghedini, M. Signoretto, F. Pinna, C. L. Bianchi, *Microchem. J.* **2014**, *112*, 186
- [14] R. Gomez, T. Lopez, J. A. Navio, A. Kubacka, M. Fernández-García, *Appl. Catal. B: Environ.* **2009**, *90*, 633–641.
- [15] M. V. Dozzi, C. D'Andrea, B. Ohtani, G. Valentini and E. Selli, *J. Phys. Chem. C* **2013**, *117*, 25586–25595.
- [16] G. Verèb, L. Manczinger, A. Oszkò, A. Sienkiewicz, I. Forró, K. Mogyorósi, A. Dombi and K. Hernádi, *Appl. Catal. B: Environ.* **2013**, *129*, 194–201.
- [17] R. Asahi, Y. Taga, W. Mannstadt, A. J. Freeman, *Phys. Rev. B* **2000**, *61*, 7459–7465.
- [18] R. Asahi, T. Moriwaka, T. Ohwaki, K. Aoki, Y. Taga, *Science* **2001**, *293*, 269–275.
- [19] C. Di Valentin, G. F. Pacchioni, A. Selloni, S. Livraghi, E. Giamello, *J. Phys. Chem B* **2005**, *109*, 85–116.
- [20] D. Li, H. Haneda, S. Hishida, N. Ohashi, *Mat. Sci. Eng. B* **2005**, *117*, 67–75.
- [21] X. Wang, S. Meng, X. Zhang, H. Wang, W. Zhong, Q. Du, *Chem. Phys. Lett.* **2007**, *444*, 292–296
- [22] E. A. Konstantinova, A. I. Kokorin, S. Saktivel, H. Kisch, K. Lips, *Chimia* **2007**, *61*, 810–814.
- [23] M. S. Wong, S. W. Hsu, K. K. Rao, C. P. Kumar, *J. Mol. Catal. A* **2008**, *279*, 20–26.
- [24] S. U.M. Kahn, M. Al-Shahry, W. B. Ingler, *Science* **2002**, *297*, 2243–2244.
- [25] R. Leary, A. Westwood, *Carbon* **2011**, *49*, 741–772.
- [26] C. S. Enache, J. Schoonman, R. van der Krol, *Appl. Surf. Sci.* **2006**, *252*, 6342–6347.
- [27] C. Xu, R. Killmeyer, L. McMahan, S. Gray, U. M. Khan, *Appl. Catal. B: Environ.* **2006**, *64*, 312–317.
- [28] H. Irie, Y. Watanabe, K. Hashimoto, *Chem. Lett.* **2003**, *32*, 772–773.
- [29] Y. Park, W. Kim, H. Park, T. Tachikawa, T. Majima, W. Choi, *Appl. Catal. B: Environ.* **2009**, *91*, 355–361.
- [30] W. Ren, Z. Ai, F. Jia, L. Zhang, X. Fan, Z. Zou, *Appl. Catal. B: Environ.* **2007**, *69*, 138–144.
- [31] Y. Li, D.-S. Hwang, N. H. Lee, S.-J. Kim, *Chem. Phys. Lett.* **2005**, *404*, 25–29.
- [32] P. Ząbek, J. Erberl, H. Kisch, *Photochem. Photobiol. Sci.* **2009**, *8*, 264–269.
- [33] D. Chen, Z. Jiang, J. Geng, Q. Wang, D. Yang, *Ind. Eng. Chem. Res.* **2007**, *46*, 2741–2746.
- [34] S. Yin, M. Komatsu, Q. Zhang, F. Saito, T. Sato, *J. Mater. Sci.* **2007**, *42*, 2399–2404.
- [35] F. Dong, W. Zhao, Z. Wu, *Nanotechnology* **2008**, *19*, 365607–365617.
- [36] Y. L. Pang, A. Z. Abdullah, *Chem. Eng. J.* **2013**, *214*, 129–138.
- [37] D. Dolat, N. Quici, E. Kusiak-Nejman, A. W. Morawski, G. Li Puma, *Appl. Catal. B: Environ.* **2012**, *115–116*, 81–89.
- [38] V. Trevisan, A. Olivo, F. Pinna, M. Signoretto, F. Vindigni, G. Cerrato, C. L. Bianchi, *Appl. Catal. B: Environ.* **2014**, *160–161*, 152–160.
- [39] D. Chen, Z. Jiang, J. Geng, Q. Wang, D. Yang, *Ind. Eng. Chem. Res.* **2007**, *46*, 2741–2746.
- [40] M. M. Joshi, N. K. Labhsetwar, P. A. Mangrulkar, S. N. Tijare, S. P. Kamble, S. S. Rayalu, *Appl. Catal. A: Gen.* **2009**, *357*, 26–33.
- [41] T. Shibata, H. Irie, M. Ohmori, A. Nakajima, T. Watanabe, K. Hashimoto, *Phys. Chem. Chem. Phys.* **2004**, *6*, 1359–1362.
- [42] M. Signoretto, E. Ghedini, V. Trevisan, C. L. Bianchi, M. Ongaro, G. Cruciani, *Appl. Catal. B: Environ.* **2010**, *95*, 130–136
- [43] J. Orth-Gerber, H. Kisch, Titanium dioxide photocatalyst containing carbon and method for its production, Patent US 2005/0226761 A1

- [44] D. A. H. Hanaor, C. C. Sorrell, *J. Mater. Sci.* **2011**, *46*, 855–874.
- [45] C. K. Choo, X. Y. Kong, T. L. Goh, G. C. Ngoh, B. A. Horri, B. Salamatinia, *Carbohydr. Polym.* **2016**, *138*, 16–26.
- [46] Y. Li, G. Ma, S. Peng, G. Lu, S. Li, *Appl. Surf. Science.* **2008**, *254*, 6831–6836.
- [47] K. Siwinska-Stefanska, J. Zdarta, D. Paukszta, T. Jesionowski, *J. Sol-Gel Sci. Technol.* **2015**, *75*, 264–278.
- [48] C. Su, B.-Y. Hong, C. M. Tseng, *Catal. Today* **2004**, *96*, 119–126.
- [49] M. Signoretto, E. Ghedini, V. Nichele, F. Pinna, D. Casotti, G. Cruciani, Valentina Aina, G. Martra, G. A. Cerrato, in *Nanoarchitectonics for Smart Delivery and Drug Targeting* (Eds.: A. M. Holban, A. Grumezescu) Elsevier, Amsterdam, **2016**, pp. 201–226.
- [50] G. A. Kloster, N. E. Marcovich, M. A. Mosiewicki, *Eur. Polym. J.* **2015**, *66*, 386–396.
- [51] I. Corazzari, R. Nisticò, F. Turci, M. G. Faga, F. Franzoso, S. Tabasso, G. Magnacca, *Polym. Degr. Stab.* **2015**, *112*, 1–9.
- [52] G. Martra, *Appl. Catal. A: General.* **2000**, *200*, 275–285.
- [53] J. Graciani, Y. Ortega, J. F. Sanz, *Chem. Mater.* **2009**, *21*, 1431–1438.
- [54] H. Kamisaka, T. Adachi, K. Yamashita, *J. Chem. Phys.* **2005**, *123*, 84704–84709.
- [55] K. Kavitha, S. Sutha, M. Prabhu, V. Rajendran, T. Jayakumar, *Carbohydr. Polym.* **2013**, *93*, 731–739.
- [56] S. Brunauer, P. H. Emmett, E. Teller, *J. Am. Chem. Soc.* **1938**, *60*, 309–319.
- [57] E. P. Barrett, L. G. Joyner, P. P. Halenda, *J. Am. Chem. Soc.* **1951**, *73*, 373–380.
- [58] M. Signoretto, E. Ghedini, V. Trevisan, C. L. Bianchi, M. Ongaro, G. Cruciani, *Appl. Catal. B: Environ.* **2010**, *95*, 130–136.
- [59] B. N. Shelimov, N. N. Tolkachev, O. P. Tkachenko, G. N. Baeve, K. V. Klemen-tiev, A. Y. Stakheev, V. B. Kazansky, *J. Photochem. Photobiol. A* **2008**, *195*, 81–88.
- [60] ISO22197-1:2007, 'Fine Ceramics, Advanced Technical Ceramics – Test Method for Air-Purification Performance of Semiconducting Photocatalytic Materials – Part 1: Removal of Nitric Oxide', ISO, Geneva, 2007.
- [61] N. Pernicone, F. Pinna, V. Trevisan, L. Cassar, G. L. Guerrini, L. Bottalico, Int. Patent, WO2011/045031A1.
- [62] B. Pereda-Ayo, U. De la Torre, M. J. Illán-Gómez, A. Bueno-López, J. R. González-Velasco, *Appl. Catal. B: Environ.* **2014**, *147*, 420–428.

Submitted: November 9, 2016

Accepted: December 23, 2016